

JMLR: Joint Medical LLM and Retrieval Training for Enhancing Reasoning and Professional Question Answering Capability

Anonymous ACL submission

Abstract

Large Language Models (LLMs) have shown significant promise in medical knowledge acquisition and question-answering. However, they can hallucinate and produce factually incorrect outcomes, even with domain-specific pretraining. Previous retrieval-augmented generation (RAG) approaches have had limited success in mitigating these hallucinations. We introduce JMLR (Jointly Trained LLM and Information Retrieval), which integrates the retriever within the LLM architecture during the fine-tuning phase. In this framework, LLM parameters are updated via cross-entropy loss, while retriever parameters are optimized using rank loss. This synchronized training enhances JMLR’s capability to retrieve clinical guidelines and leverage medical knowledge for reasoning and answering questions, all while reducing computational demands. We evaluated JMLR on a critical medical question-answering application, demonstrating that JMLR-13B (70.5%) outperforms the previous state-of-the-art model, Meditron-70B (68.9%), and Llama2-13B with RAG (67.7%) on a medical question-answering dataset. Furthermore, in the USMLE factuality score assessed by GPT-4, JMLR showed a greater reduction in hallucinations (0.2463) compared to Claude3 Haiku (0.2337), Claude3 Opus (0.2356), and GPT-3.5 (0.2187). Comprehensive evaluations indicate that JMLR-13B improves reasoning quality and effectively reduces hallucinations. Additionally, JMLR-13B trains significantly faster (148 GPU hours) than Meditron-70B (42630 GPU hours). This work offers a novel and efficient knowledge enhancement method for healthcare, highlighting the potential of integrating retrieval and LLM training for medical question-answering systems.¹

1 Introduction

Effective clinical decision-making relies on a logical diagnostic chain, which requires specialized

¹We will release code and data set soon.

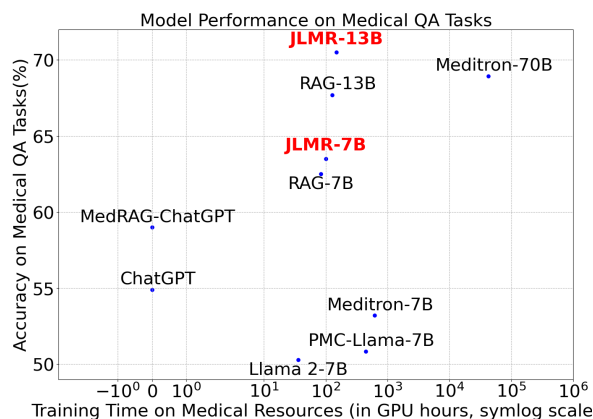


Figure 1: JMLR achieved the highest average accuracy across the MMLU-Medical, MedMcQA, MedQA, and Amboss datasets, utilizing only 148 GPU hours.

knowledge that isn’t widely accessible, presenting a major healthcare challenge. Large Language Models (LLMs) show promise in making this critical medical knowledge more accessible (Peng et al., 2023; Yang et al., 2023). Traditionally, LLMs have been developed for general tasks using data from diverse online sources, leading to a lack of high-quality, domain-specific information, especially in medicine (Wornow et al., 2023; Singhal et al., 2023a). Previous researches expand medical knowledge by continuing training general domain LLMs with domain-specific datasets. (Yunxiang et al., 2023; Zhang et al., 2023; Toma et al., 2023).

However, LLMs face the significant challenge of “hallucination”, where models generate plausible but incorrect or unverified information (Ji et al., 2023; Bang et al., 2023). Such errors raise serious concerns in healthcare, where accuracy is imperative (Ahmad et al., 2023). Hence, recent works proposed retrieval augmented generation (RAG): they first train a retriever to obtain relevant documents from a general domain corpus based on the input query and then train an LLM to generate a response based on the input query and the retrieved documents (Lewis et al., 2020; Borgeaud

et al., 2022a; Cheng et al., 2023; Hiesinger et al., 2023; Xiong et al., 2024). By retrieving domain-specific documents, RAG identifies relevant knowledge and provides contextual grounding for LLMs, thereby alleviating hallucination issues (Shuster et al., 2021; Zhu et al., 2023).

Although RAG shows high accuracy in benchmarks for open-domain question answering, its effectiveness in specific domains is yet in challenge because retrievers trained in the general domain usually perform worse than those fine-tuned in the specific domain (Gao et al., 2023; Zhao et al., 2022; Thakur et al., 2021). Fine-tuning retrievers requires document-query pairs, which may not be readily available for a specific domain. Labeling such medical pairs specifically for this purpose incurs additional time and financial costs. Moreover, RAG trains retriever and LLM separately. When training LLM with a frozen retriever, the retrieval may not be optimized to align with LLM to produce the correct answer (Asai et al., 2024; Yoran et al., 2023; Rubin et al., 2022). In this study, we introduce a novel method to jointly train retrieval and LLM. Although the method is generalizable, we focus on evaluating it in the medical domain, where the accuracy of the generated content is crucial.

Specifically, we introduce Joint Medical LLM and Retrieval Training (JMLR), a novel approach that jointly train LLM and retriever. As shown in Figure 2, JMLR presents a novel approach compared to the traditional pretrain-finetune process. JMLR enhances question answering by fetching relevant domain-specific documents that maximize the potential of LLMs. This involves including each retrieved document in the initial input question before the LLM’s response attempt, thereby augmenting the input to train the LLM for answer generation. For training jointly, JMLR introduces a unique mechanism called LLM-Rank loss to train the retriever. This is achieved by evaluating the improvement in LLM’s performance upon including any candidate retrieved documents. We calculate the log probability of the LLM’s answer with each candidate, adopting the negative of these values as the relevance score for each candidate. When reducing this loss, the retriever is trained to prioritize candidate documents that significantly aid the LLM. Our results show that the joint training improves medical question answering, especially in scenarios requiring nuanced understanding and specific information retrieval.

To validate JMLR’s effectiveness in reducing computational resource requirements and fully utilizing given knowledge, we designed three experimental setups. These experiments evaluated whether direct fine-tuning, instead of traditional pretraining, would improve JMLR’s performance. We utilized external data resources for retrieval, including the MIMIC-IV dataset (Johnson et al., 2020), medical textbooks, and diverse medical documents for knowledge expansion. We experimented with different LLMs, including PMC-Llama, Meditron, GPT-3.5 with or without MedRAG (Wu et al., 2023; Chen et al., 2023b; Achiam et al., 2023). Our JMLR-7B has demonstrated superior results, achieving an impressive 62.3% accuracy, outperforming the traditional method’s 53.2% on the medical QA dataset. Our 13B model (70.5%) surpasses the performance of both the open-source medical LLM (Meditron 70B: 68.9%) and closed-source general LLM (GPT-3.5: 54.9%). Furthermore, to demonstrate the effectiveness of our approach in reducing hallucination, we conducted evaluations using the UMLS factuality score and GPT-4 score. Our method was compared against several SOTA models, including Claude3 Haiku, Claude3 Opus, and GPT-3.5. The results indicate that our model outperforms the others, with scores of UMLS factuality: 0.2463 and GPT-4: 4.3036, compared to GPT-3.5 (UMLS factuality: 0.2187, GPT-4: 4.0620), Claude3 Haiku (UMLS factuality: 0.2337, GPT-4: 4.0559), and Claude3 Opus (UMLS factuality: 0.2356, GPT-4: 4.3449). Moreover, evaluation by domain experts supports the superior performance of JMLR. We summarize our key contributions as follows:

- We propose a novel method that jointly trains retrieval and LLMs, resulting in JMLR-13B surpassing the state-of-the-art 70B open-source model in several medical question-answering benchmarks.
- Through comprehensive automated and human evaluations, we demonstrate that JMLR-13B consistently enhances models’ reasoning quality while significantly reducing hallucinations, achieving superior reasoning ability compared to Claude3-Opus.
- JMLR shows promise to enhance domain-specific retrieval by fully eliminating additional human annotation.

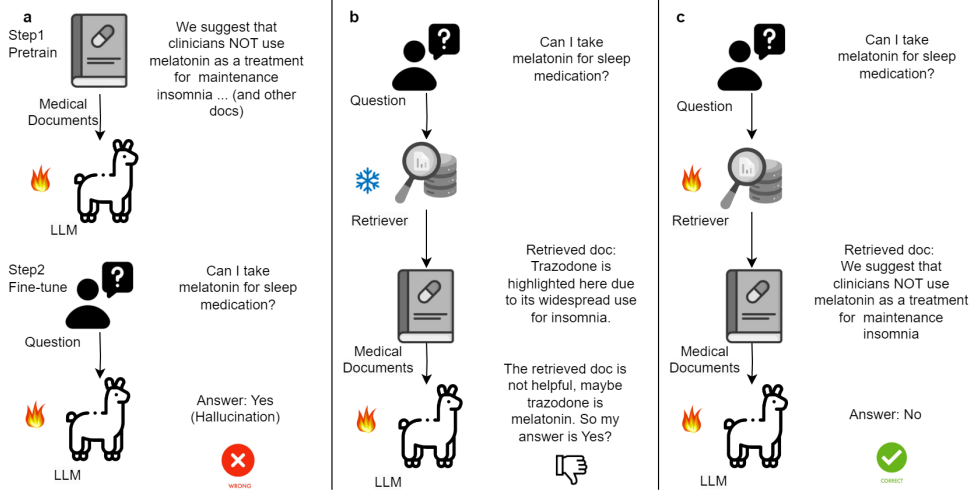


Figure 2: Comparison between different domain adaptation methods: traditional domain pretraining method (left), RAG (middle), and JMLR (right). JMLR retrieves the documents to reduce the hallucination. Parameters are updated simultaneously for the retriever and large language models (LLM) models, leading the retriever to know which domain-specific document is helpful for LLM to give a reasonable answer.

- To train 7B model with domain specific knowledge, our JMLR achieve a better computation efficiency with 100 GPU hours. This is a considerable reduction compared to Meditron’s pretrain-finetune process, where pretraining alone takes 588 hours, and finetuning adds an additional 36 hours.

2 Problem Formulation & Traditional Method

Given a set of medical questions \mathcal{Q} and a set of medical documents \mathcal{D} containing medical knowledge, our goal is to construct a language model \mathcal{M} that can provide accurate answers.

Formally, for each question $q_i \in \mathcal{Q}$, there is a corresponding correct answer a_i^* within a set of options A_i , where $a_i^* \in A_i$. The model \mathcal{M} maps each question to a predicted answer:

$$\hat{a}_i = \mathcal{M}(q_i, \mathcal{D}; \theta)$$

where θ represents the parameters of the model.

Our objective is to find the optimal parameters θ^* that minimize the loss function \mathcal{L} , which measures the discrepancy between the predicted answer \hat{a}_i and the correct answer a_i^* :

$$\theta^* = \arg \min_{\theta} \sum_{i=1}^{|\mathcal{Q}|} \mathcal{L}(\hat{a}_i, a_i^*)$$

The loss function can be instantiated as a cross-entropy loss for classification tasks, where the number of classes is equal to the number of options.

To solve this problem, previous methods pre-trained LLM to learn medical knowledge for a medical LLM, and then finetuned medical LLM on medical QA task (Chen et al., 2023b; Wu et al., 2023; Yunxiang et al., 2023; Toma et al., 2023). Specifically, such traditional pretrain-finetune pipeline first continued pretraining general domain LLMs on medical documents \mathcal{D} with next-token prediction loss function, and then finetuned the medical LLMs to select a_i^* given question q_i and option description with loss function \mathcal{L} .

3 Method

In comparison to traditional method, JMLR did not pretrain LLM on medical documents. Instead, JMLR selected question-related medical documents as additional context during fine-tuning of an open-domain LLM. Specifically, given a question q_i , we trained retriever to find helpful medical documents from \mathcal{D} , which was then used to train LLM to generate the final answer a_i^* .

3.1 Retriever

For information retrieval, we adopted the **ColBERT** model (Santhanam et al., 2021), using its pre-trained weights as initialization. ColBERT employs BERT-based encoders to independently transform both queries and documents into bags of embeddings. A single BERT model is shared between the query and document encoders, but the inputs are differentiated using special tokens: $[Q]$ for queries and $[D]$ for documents. For a query $q = q_0 q_1 \dots q_l$, the input is tokenized into

BERT’s WordPiece tokens, and the sequence is formatted as $[CLS] [Q] q_0q_1 \dots q_l$. For documents $d = d_0d_1 \dots d_n$, the input sequence is similarly tokenized and formatted as $[CLS] [D] d_0d_1 \dots d_n$. Both the padded query and document token sequences are passed through BERT, followed by subsequent processing to compute embeddings E_q and E_d . Specifically:

$$E_q := \text{CNN}(\text{BERT}([Q]q_0q_1 \dots q_l))$$

$$E_d := \text{Filter}(\text{CNN}(\text{BERT}([D]d_0d_1 \dots d_n)))$$

$$S_{q,d} := \sum_{i \in [|E_q|]} \max_{j \in [|E_d|]} E_{q_i} \cdot E_{d_j}^T$$

Here, E_q represents the normalized embeddings for queries, processed through a CNN layer applied to BERT’s output. For documents, E_d follows the same normalization and CNN steps but includes an additional filtering operation to remove embeddings corresponding to punctuation tokens, as determined by a predefined list. This filtering reduces unnecessary embeddings and ensures more effective document representations.

3.2 LLM

We adapted Llama as our LLM model. The original Llama model (Touvron et al., 2023) supports only a maximum of 4k tokens, which poses a challenge when multiple documents are retrieved. To address this, we utilized the Shifted Sparse Attention (S2-Attn) mechanism (Chen et al., 2023a), which can be used to process long sequences by mitigating the high memory cost and slow processing time associated with standard self-attention in LLMs. S2-Attn divides input into sequence spans within self-attention modules and introduces shifted patterns for inter-span information exchange. This extends context length efficiently without extra computational costs and achieves near-baseline performance.

3.3 JMLR Architecture

However, Colbert matches queries and documents based on the retriever similarity not helpful, returning scores and documents. To enable the retriever system to return documents that are more helpful for providing accurate answers to Llama, we constructed the JMLR architecture. Let \mathcal{Q} be a set of queries, \mathcal{D} be a corpus of domain-specific documents, and \mathcal{Y} be the ground truth answers (y_1, y_2, \dots) for queries. Our task is to construct a function f parameterized by θ , which generates an

answer $\hat{Y} \in \hat{\mathcal{Y}}$ based on questions $Q \in \mathcal{Q}$ and a set of documents $D \subseteq \mathcal{D}$.

The objective is to simultaneously learn the optimal parameters θ^* and ϕ^* that minimize the combined loss on the retrieved documents and the generated answers, formalized as: $(\theta^*, \phi^*) = \arg \min_{\theta, \phi} \mathbb{E}_{(Q, Y) \sim \mathcal{T}} [\mathcal{L}(f_Y(Q, f_R(Q; \phi), \theta), Y)]$ where \mathcal{L} is a loss function that evaluates the correctness of the answer and the helpfulness of the retrieved documents. The retrieval function f_R is defined by:

$$f_R(Q; \phi) = \arg \top_{D \subseteq \mathcal{D}, |D|=k} S_{q,d}(Q, D; \phi)$$

and the similarity function $S_{q,d}(Q, D; \phi)$ scores how relevant each document D is to the question Q .

The combined optimization involves updating both θ and ϕ through gradient descent to minimize the expected loss:

$$\nabla(\theta, \phi) \propto \nabla_{\theta, \phi} \mathcal{L}(f_Y(Q, f_R(Q; \phi), \theta), Y)$$

where $\nabla_{\theta, \phi} \mathcal{L}$ denotes the gradient of the loss function with respect to both sets of parameters. This dual-parameter optimization ensures that the retrieval function is aligned with the needs of the answer function, enhancing both the accuracy of the responses and the relevance of the information retrieved.

To solve this, the JMLR architecture employs a rank loss, L_{rank} , to link the LLM and retriever systems. The content quality generated by the LLM influences the retriever’s parameter updates. Specifically, if a returned document D_i reduces the LLM’s loss function \hat{L} more than another document D_j , it indicates that D_i is more helpful for answering the query than D_j . Correspondingly, the retriever’s scoring function should assign a higher score to D_i . Our rank loss ensures alignment between the LLM’s loss and the retriever’s scoring function: documents that contribute to lower LLM loss receive higher scores.

Since the scoring function is computed by the retriever, we use the rank loss to update both the LLM and retriever simultaneously based on the gradient $\nabla(\theta, \phi)$. To address the large variance in scores generated by the retriever, we normalize them to obtain \hat{S} .

$$\mathcal{L} = L_{\text{rank}} + L(f_Y(Q, f_R(Q; \phi)), \theta, Y),$$

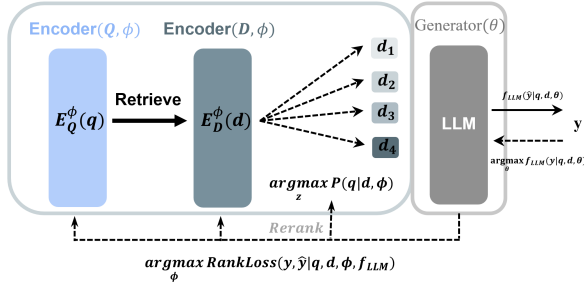


Figure 3: Overview of the JMLR architecture. Unlike traditional retrieval-augmented generation (RAG) models, which separately optimize the retriever and the LLM, our approach jointly trains both components by minimizing a combined loss. Specifically, the retriever scores candidate documents based on their relevance to the query Q using the similarity function $S_{q,d}(Q, D; \phi)$. The top k documents are retrieved and passed to the LLM to generate answers \hat{Y} . A rank loss L_{rank} is employed to align the retriever’s scoring function with the LLM’s loss function. Documents that contribute to reducing the LLM’s loss are assigned higher scores by the retriever. This joint optimization ensures that the retriever provides documents that are more helpful for answer generation, while the LLM learns to utilize relevant documents effectively. The dynamic selection of documents further enhances robustness by exposing the LLM to both useful and irrelevant documents, enabling it to discern and integrate useful knowledge more effectively.

where L_{rank} is defined as:

$$L_{\text{rank}} := -\frac{1}{M} \sum_{i=1}^M \mathbb{I}(L_i \neq 0) \cdot F_i,$$

where M is the number of queries in the training set, and F_i is calculated as:

$$F_i = \mathbb{I}(L_i) \log(C_i) + (1 - \mathbb{I}(L_i)) \log(1 - C_i).$$

Here, C_i represents the contrastive logits, defined as:

$$C_i = \text{Normalize}(S_{q_i, d_k}) - \text{Normalize}(S_{q_i, d_j}),$$

where S_{q_i, d_k} and S_{q_i, d_j} are the similarity scores assigned to documents d_k and d_j , respectively.

We define $y'(q, d_j)$ as the answer generated by the LLM for query q based on the retrieved document d_j . The decision-based loss differences are calculated as:

$$L_i = \hat{L}_i(y, y'(q, d_j)) - \hat{L}_j(y, y'(q, d_k)).$$

For JMLR training, the dataset consists of question-answer (QA) pairs, where the input is a question and the output includes the correct answer

and rationale. During training, the top 7 documents with the highest scores are aggregated and fed into the model. Initially, we extract the top 30 documents based on the retriever’s scores. In each iteration, these scores are used for weighted random sampling, where documents with higher scores have a greater likelihood of selection. This ensures that the set of documents inputted into the LLM varies dynamically. By exposing the LLM to both useful and irrelevant documents, this approach enhances its robustness, enabling it to better discern relevant knowledge from noisy information.

4 Experiment

4.1 Dataset

Medical document and Benchmark: Data quality of medical documents is important for LLMs to answer medical questions. Previous work primarily sourced from a wide array of medical research articles and clinical guidelines. Research papers, like those found in PubMed, provide foundational and current information on healthcare. Clinical guidelines are thoroughly designed protocols developed to assist clinicians in making decisions given patient medical history. Other high-quality medical documents to retrieve include medical textbooks.

Medical Benchmark: The MedQA dataset (Jin et al., 2021), sourced from the official USMLE website, includes questions for Step 1, Step 2 CK, and Step 3, reflecting the complex medical knowledge and ethical scenarios faced by medical students and practitioners from June 2022 to March 2023. The Amboss question bank enhances our training material with diverse questions for the same exams. The MedMCQA dataset comprises 194,000 multiple-choice questions from Indian medical entrance exams, covering 2,400 healthcare topics across 21 medical subjects (Pal et al., 2022). Additionally, MMLU-Medical, selected from the MMLU dataset (Hendrycks et al., 2020), focuses on nine key subjects relevant to medical knowledge. Lacking a training set, we evaluate this dataset using an LLM originally trained on MedMCQA, applying supervised fine-tuning to each QA dataset and assessing their performance on the corresponding test sets, with MedQA and Amboss providing detailed rationales. Details are shown in Appendix 10.2.

4.2 Evaluation Metrics

For automated metrics, we used accuracy to evaluate the model’s ability to select the correct final

Model	MedQA	Amboss	MMLU-M	MedMCQA	AVG
GPT-3.5	50.2	49.1	69.4	51.0	54.9
GPT-4	74.7	82.1	88.4	69.5	78.6
Meditron-70B	60.7	76.4	73.6	65.1	68.9
RAG-13B	59.9	76.9	69.9	64.2	67.7
JMLR-13B	62.5	81.2	72.8	65.5	70.5

Table 1: Comparison between JMLR and SOTA open (Meditron, RAG, JMLR) or closed (GPT-3.5/4) LLMs.

choice. We evaluated the rationale quality using metrics UMLS-F and GPT-4 score. UMLS-F is a factuality metric based on F1 score between entities in gold explanation and generated explanation². GPT-4 score is a reference-free metric. GPT-4 was asked to rate the generated explanation on a Likert scale from 1 to 5 (higher better) along the 3 dimensions: question comprehension (e.g., indication the question has been understood), recall of knowledge (e.g., mention of a relevant and/or correct fact for answering the question), and medical reasoning (e.g., correct reasoning for answering the question) (Singhal et al., 2023a). We put GPT-4-score prompts in Table 9.

For human evaluation, we engaged three medical professionals to review and assess a small sample of 50 questions drawn from the test sets. These doctors were asked to provide their preference for the rationales generated by two models (GPT-3.5 and JMLR-13b) given the gold rationale.

To validate the reliability of the selected automated metrics, we calculated the Cohen’s Kappa between UMLS-F and expert preference, as well as Kappa between the GPT-4 score and expert preference, obtaining results of 0.69 and 0.81, respectively. These results indicate that both metrics exhibit substantial to almost perfect agreement with human evaluation.

5 Main Results

As shown in Table 1, our JMLR with 13B parameters outperforms previous SOTA open access model Meditron 70B parameters and even closed access model such as GPT-3.5.

5.1 Domain Retrieval > Domain Pretrain

Domain retrieval models (both RAG-7B and our JMLR-7B) outperform domain-pretrained LLMs across all medical QA benchmarks, as shown in Table 2. In the MedQA and Amboss datasets, where JMLR-7B not only outperforms baselines but does so with a notable margin, scoring 51.3% in MedQA

²More UMLS-F details can be found in Appendix 10.8

Model	MedQA	Amboss	MMLU-M	MedMCQA	AVG
Llama 2	44.0	46.5	56.3	54.4	50.3
Meditron*	47.9	50.1	55.6	59.2	53.2
RAG#	47.3	50.7	63.8	62.1	55.9
JMLR#	51.3	68.3	65.3	64.1	62.3

Table 2: Comparison between domain retrieval (#) and domain pretraining (*) using models of the same 7B size and domain data (Open Guidelines).

and 68.3% in Amboss. This is particularly significant when compared to Meditron-7B, which scores 47.9% and 50.1% in these datasets, respectively. The trend continues in MMLU-Medical and MedMCQA datasets, JMLR-7B achieved scores of 65.3% and 64.1%, surpassing the scores of Meditron-7B (55.6% and 59.2%). Overall, the results illustrate that JMLR-7B model, on average, achieves about a 17% improvement in performance over its closest competitor, Meditron-7B. This highlights the effectiveness of our training method and the substantial advancements it brings to the field of medical benchmarking.

The enhanced performance of JMLR-7B can be partially attributed to its use of Llama-2 as the foundational model, showcasing significantly higher average performance than other pre-trained baselines. However, the distinct edge comes from our integrated training approach that combines retriever and LLM. This methodology not only further enhances Llama-2’s performance in medical benchmarks but also equips the retriever component with the ability to effectively source relevant and beneficial documents to aid the LLM in answering questions. In contrast, GPT-3.5, when devoid of medical guidelines, has been known to make basic mistakes, such as recommending vaccinations to pregnant women—a practice that contradicts medical norms as documented in Table 7. Our model, with the support of guidelines, avoids such errors. This synergistic approach substantially reduces hallucinations and bolsters the model’s overall reliability.

5.2 Joint Training > RAG

During fine-tuning, synchronously updating both the Retriever and LLM yields better results than updating only the LLM. Table 1 shows that JMLR models significantly outperform traditional RAG methods. For example, JMLR-13B’s scores (72.8% on MMLU, 65.5% on MedMcQA) is far superior to RAG-13B (69.9% on MMLU, 64.2% on MedMCQA). This result suggests that without updating the retriever, the documents retrieved may be rele-

vant to the question but not necessarily helpful to the LLM’s response. Joint training ensures that the retriever learns which documents are beneficial for LLM. To evaluate the adaptability of the JMLR retriever, we further applied it to other LLMs. Specifically, we employed different retrievers to identify relevant documents, which were then provided to GPT-3.5 for generating the final answer. The retriever trained with JMLR attained an average accuracy of 57.5%, while the retriever from RAG achieved an accuracy of 56.7%. In addition, we present a case study in Table 7, where JMLR retrieves closely related cases. These results indicate that the JMLR retriever effectively identifies documents that not only support Llama but also aid GPT-3.5 in selecting the correct answers.

5.3 Enhancing Model Rationale Quality

	Haiku	Opus	GPT3.5	JMLR
UMLS Factuality	0.2337	0.2356	0.2187	0.2463
GPT-4 Overall	4.0559	4.2449	4.0620	4.3036
GPT-4 Comprehension	4.7107	4.7561	4.7549	4.7661
GPT-4 Reasoning	3.6701	4.0976	3.6863	4.0101
GPT-4 Recall	3.6726	3.8780	3.6849	4.1661

Table 3: UMLS-F and GPT-4 score across 4 different models (e.g., Claude3, GPT3.5, JMLR-13B).

In addition to significantly improving the model’s performance in QA accuracy, JMLR also plays a crucial role in helping the model generate higher-quality rationales with fewer hallucinations. As shown in the Table 3, both UMLS Factuality and GPT-4 Overall scores show that JMLR-13B outperforms the other three models, demonstrating its high-quality rational generation. This result aligns with our expert evaluations on the small samples, where JMLR-13B achieved a win rate of 0.61 compared to GPT-3.5.

Specifically, GPT-4 Comprehension primarily measures the plausibility of generated reasons. As shown in Table 3, the scores for GPT-4 Comprehension are uniformly high across all models, with only minor differences, indicating that all these models can generate logically coherent explanations for the questions. GPT-4 Reasoning evaluates medical logical reasoning abilities. JMLR-13B stands out in this criteria because its retrieval guidelines include valuable content, such as information on Differential Diagnosis, which aids the model in more effectively associating key information like symptoms, diseases, and medications presented in the questions. Finally, GPT-4 Recall assesses factuality, i.e., whether the model can hit the critical information

points. Our results demonstrate that JMLR-13B achieves the most significant improvement in this criteria. The high-quality documents retrieved by JMLR-13B provide the necessary key information, allowing the model to generate higher-quality rationales around these key points. The assessments of UMLS Factuality are similar to GPT-4 Recall, and their final results are consistent. We further explore this in the appendix 10 and provide case studies to support our findings.

6 Ablation Study

	MedQA	Amboss
FT-Llama-7B	44.0	46.5
FT-Llama-7B-ColBERT	40.6	45.6
JMLR-7B-Separate	55.3	69.0
JMLR-7B	56.2	71.2

Table 4: We conducted an ablation study to verify the necessity of the JMLR training method. We discussed retrieval versus no retrieval and asynchronous training versus joint training. Ultimately, we found that the JMLR training method significantly outperformed the other approaches.

To assess the effects of fine-tuning and information retrieval on QA accuracy, we compare *JMLR-7B* (on medical documents) with the following new baselines: The *JMLR-7B-Separate* model updates the parameters of both Llama and the retriever similar to *JMLR-7B*, but in an asynchronous manner. Initially, it fixes the parameters of the retriever while only updating those of Llama. Subsequently, it reverses this process, updating only the retriever’s parameters using rank loss. The *FT-Llama-7B+ColBERT* model, on the other hand, freezes the retriever in a manner akin to *RAG-7B*. However, the retriever in this setup is solely applied during inference and not during fine-tuning. The *FT-Llama-7B* serves as a naive fine-tuned baseline where the retriever is not employed. We fine-tuned the Llama 2-7B on the training sets. The accuracy are shown in Table 4. From the table, we can observe that:

- *FT-Llama-7B+ColBERT* (44.0% on MedQA, 46.5% on Amboss) showed significant improvements over *FT-Llama-7B*, indicating that the fine-tuning phase notably enhanced Llama’s capabilities in medical QA. However, this phase did not effectively leverage medical guidelines.
- *JMLR-7B-Separate* model achieved superior performance (55.3% on MedQA and 69.0%

on Amboss), surpassing the *FT-Llama-7B-ColBERT* (40.6% on MedQA, 45.6% on Amboss). The distinctive fine-tuning approach of *JMLR-7B-Separate*, which integrates medical documents during the tuning phase, enables the model to utilize medical resources more effectively.

- *JMLR-7B* (56.2% on MedQA, 71.2% on Amboss) uses a joint training approach that facilitates the retrieval of highly relevant medical documents, surpassing the *JMLR-7B-Separate* (55.3% on MedQA, 69.0% on Amboss). The result demonstrate that jointly training(update the whole parameters in every step) Llama and ColBERT outperforms training the two separately(such as REALM training method).

7 Related Work

Medical Large Language Model Medical LLMs have evolved from adapting models like BERT with biomedical datasets (Gu et al., 2021; Lee et al., 2020) to incorporating knowledge graphs (Yasunaga et al., 2022). Architectures such as GPT (Bubeck et al., 2023) and Llama (Touvron et al., 2023) have been trained on domain-specific (Wu et al., 2023; Gema et al., 2023; Yunxiang et al., 2023; Zhang et al., 2023; Labrak et al., 2024) or synthetic data (Tran et al., 2023; Han et al., 2023; Kweon et al., 2023). Recent advancements have scaled up data and model parameters, resulting in models like GatorTronGPT (Peng et al., 2023) and Clinical-Camel (Toma et al., 2023), alongside research on Flan-PaLM and PaLM-2’s medical reasoning using chain-of-thought (Singhal et al., 2023a,b; Wei et al., 2022; Wang et al., 2022). Additionally, Meditron (Chen et al., 2023b), an open-source medical LLM suite with 7B and 70B parameters, demonstrates superior performance against leading benchmarks and comparable results to GPT-3.5 and Med-PaLM-2. However, performance gains have plateaued despite increased model size, failing to effectively address model forgetting (Wang et al., 2023; Luo et al., 2023). To counter this, our study integrates a retriever with LLMs during training, offering 7B and 13B versions that outperform traditional pre-trained models, with our 13B model exceeding even Meditron 70B.

Retrieval-Augmented Language Models In the clinical domain, LLMs’ factual inaccuracies pose

significant risks, such as misdiagnoses (Petroni et al., 2019; Sung et al., 2021; Yao et al., 2022; Singhal et al., 2023a). Integrating external knowledge repositories enhances LLM performance across NLP tasks (Min et al., 2022). Traditional retrieval-augmented generation (RAG) models rely on static retrieval components that often fail to integrate documents effectively (Yu, 2022; Izacard et al., 2022). Innovations like Atlas (Izacard et al., 2022) and RETRO (Borgeaud et al., 2022b) have advanced the use of external data, but challenges persist in blending this information with LLM outputs. Some methods, like REALM (Guu et al., 2020), REPLUG (Shi et al., 2023), and RA-DIT (Lin et al., 2023), attempt to enhance document relevance by training unsupervised retrievers. However, these systems often lack fully synchronized training between the retriever and the LLM. For example, REALM updates the retriever intermittently after training the LLM for fixed steps, while REPLUG focuses solely on retriever optimization, freezing the LLM parameters. Atlas and RA-DIT only update the query encoder in the retriever. These approaches fail to jointly optimize the retriever and LLM as a unified system. In contrast, our method synchronizes the training of both the retriever and LLM end-to-end, ensuring the retriever dynamically aligns with the LLM’s evolving outputs. This joint optimization boosts document relevance and external knowledge integration. Experiments demonstrate that our approach outperforms traditional stepwise methods, achieving superior performance.

8 Conclusion

This study introduces JMLR framework, significantly enhancing performance in medical QA and reasoning tasks. The JMLR models not only outperform existing state-of-the-art models in efficiently handling medical resources but also effectively reduce hallucinations in information generation, improving the accuracy and reliability of answers and explanations. Experimental results demonstrate substantial performance improvements across multiple medical benchmark tests, validating the effectiveness of integrating retriever and language model training. Furthermore, the reasoning capabilities of the JMLR model have been recognized by both GPT-4 and medical professionals, further confirming its potential and reliability.

9 Limitations and Ethical Considerations

This study offers valuable insights but also comes with several limitations that we would like to highlight:

- **Domain Specificity:** Our research exclusively focuses on the task of medical QA and reasoning. The adaptation of the proposed method to other domains remains unexplored. This suggests that our approach may need further validation and adjustments before being applied to different fields.
- **Expertise of Annotators:** We relied on 3 doctors as annotators for human evaluation and preference results. While they are qualified to provide expert medical opinions and insights, employing more qualified domain experts as annotators would enhance the statistical significance of our results. We leave this to future work, along with addressing concerns about fairness, generalizability to other domains/languages, and potential biases inherent in LLMs.

Privacy Implications Despite significant advancements in the performance of medical knowledge acquisition and question-answering systems, privacy protection becomes a paramount concern when dealing with sensitive medical data. In particular, our model utilizes data from textbooks and public guideline.

Bias Considerations Furthermore, while we strive to enhance the model’s performance across multiple medical question-answering datasets, we must acknowledge that the choice and composition of datasets could introduce or exacerbate biases within the model. For example, if training data predominantly comes from certain geographic locations or populations, the model might exhibit biases towards medical conditions or treatment methods outside those groups. This could limit the fairness and effectiveness of the model when applied globally. Future research should consider training with more diverse and comprehensive datasets to reduce potential biases and enhance the model’s universal applicability.

Broader Impacts Our study represents an important step forward in advancing AI applications in the field of medicine, but its broader societal

impacts also require careful consideration. In particular, automated medical question-answering systems hold great potential in improving healthcare efficiency and accuracy but could also impact the roles of medical professionals and patient care practices. For instance, reliance on these systems may sometimes reduce direct communication between doctors and patients or might influence physicians’ clinical judgment. Therefore, implementing these technological solutions should be approached with caution, ensuring they serve as a complement, not a replacement, to the toolkit of medical professionals. Moreover, the public’s understanding and acceptance of these systems are crucial for their widespread use, necessitating enhanced education and transparency.

In summary, while our research demonstrates the potential of leveraging large language models and information retrieval techniques in medical question-answering systems, close attention must be paid to the ethical considerations of privacy, bias, and broader societal impacts. Future work should aim to address these challenges, ensuring the development and application of these technologies benefit the healthcare system and society as a whole.

706
707
708
709
710
711

712
713
714
715

716
717

718
719
720
721

722
723
724
725
726
727

728
729
730
731

732
733
734
735
736
737
738
739
740
741
742
743
744
745
746

747
748
749
750
751
752
753

754
755
756
757
758
759

References

Josh Achiam, Steven Adler, Sandhini Agarwal, Lama Ahmad, Ilge Akkaya, Florencia Leoni Aleman, Diogo Almeida, Janko Altenschmidt, Sam Altman, Shyamal Anadkat, et al. 2023. Gpt-4 technical report. *arXiv preprint arXiv:2303.08774*.

Muhammad Aurangzeb Ahmad, Ilker Yaramis, and Taposh Dutta Roy. 2023. Creating trustworthy llms: Dealing with hallucinations in healthcare ai. *arXiv preprint arXiv:2311.01463*.

AI Anthropic. 2024. The claude 3 model family: Opus, sonnet, haiku. *Claude-3 Model Card*.

Akari Asai, Zexuan Zhong, Danqi Chen, Pang Wei Koh, Luke Zettlemoyer, Hannaneh Hajishirzi, and Wen tau Yih. 2024. [Reliable, adaptable, and attributable language models with retrieval](#).

Yejin Bang, Samuel Cahyawijaya, Nayeon Lee, Wenliang Dai, Dan Su, Bryan Wilie, Holy Lovenia, Ziwei Ji, Tiezheng Yu, Willy Chung, et al. 2023. A multi-task, multilingual, multimodal evaluation of chatgpt on reasoning, hallucination, and interactivity. *arXiv preprint arXiv:2302.04023*.

Olivier Bodenreider. 2004. The unified medical language system (umls): integrating biomedical terminology. *Nucleic acids research*, 32(suppl_1):D267–D270.

Sebastian Borgeaud, Arthur Mensch, Jordan Hoffmann, Trevor Cai, Eliza Rutherford, Katie Millican, George Bm Van Den Driessche, Jean-Baptiste Lespiau, Bogdan Damoc, Aidan Clark, Diego De Las Casas, Aurelia Guy, Jacob Menick, Roman Ring, Tom Hennigan, Saffron Huang, Loren Maggiore, Chris Jones, Albin Cassirer, Andy Brock, Michela Paganini, Geoffrey Irving, Oriol Vinyals, Simon Osindero, Karen Simonyan, Jack Rae, Erich Elsen, and Laurent Sifre. 2022a. [Improving language models by retrieving from trillions of tokens](#). In *Proceedings of the 39th International Conference on Machine Learning*, volume 162 of *Proceedings of Machine Learning Research*, pages 2206–2240. PMLR.

Sebastian Borgeaud, Arthur Mensch, Jordan Hoffmann, Trevor Cai, Eliza Rutherford, Katie Millican, George Bm Van Den Driessche, Jean-Baptiste Lespiau, Bogdan Damoc, Aidan Clark, et al. 2022b. [Improving language models by retrieving from trillions of tokens](#). In *International conference on machine learning*, pages 2206–2240. PMLR.

Sébastien Bubeck, Varun Chandrasekaran, Ronen Eldan, Johannes Gehrke, Eric Horvitz, Ece Kamar, Peter Lee, Yin Tat Lee, Yuanzhi Li, Scott Lundberg, et al. 2023. Sparks of artificial general intelligence: Early experiments with gpt-4. *arXiv preprint arXiv:2303.12712*.

Yukang Chen, Shengju Qian, Haotian Tang, Xin Lai, Zhijian Liu, Song Han, and Jiaya Jia. 2023a. Longlora: Efficient fine-tuning of long-context large language models. *arXiv preprint arXiv:2309.12307*.

Zeming Chen, Alejandro Hernández Cano, Angelika Romanou, Antoine Bonnet, Kyle Matoba, Francesco Salvi, Matteo Pagliardini, Simin Fan, Andreas Köpf, Amirkeivan Mohtashami, et al. 2023b. Meditron-70b: Scaling medical pretraining for large language models. *arXiv preprint arXiv:2311.16079*.

Xin Cheng, Di Luo, Xiuying Chen, Lemao Liu, Dongyan Zhao, and Rui Yan. 2023. [Lift yourself up: Retrieval-augmented text generation with self memory](#). *ArXiv*, abs/2305.02437.

Yunfan Gao, Yun Xiong, Xinyu Gao, Kangxiang Jia, Jinliu Pan, Yuxi Bi, Yi Dai, Jiawei Sun, Qianyu Guo, Meng Wang, and Haofen Wang. 2023. [Retrieval-augmented generation for large language models: A survey](#). *ArXiv*, abs/2312.10997.

Aryo Gema, Luke Daines, Pasquale Minervini, and Beatrice Alex. 2023. Parameter-efficient fine-tuning of llama for the clinical domain. *arXiv preprint arXiv:2307.03042*.

Yu Gu, Robert Tinn, Hao Cheng, Michael Lucas, Naoto Usuyama, Xiaodong Liu, Tristan Naumann, Jianfeng Gao, and Hoifung Poon. 2021. Domain-specific language model pretraining for biomedical natural language processing. *ACM Transactions on Computing for Healthcare (HEALTH)*, 3(1):1–23.

Kelvin Guu, Kenton Lee, Zora Tung, Panupong Pasupat, and Mingwei Chang. 2020. Retrieval augmented language model pre-training. In *International conference on machine learning*, pages 3929–3938. PMLR.

Tianyu Han, Lisa C Adams, Jens-Michalis Papaioannou, Paul Grundmann, Tom Oberhauser, Alexander Löser, Daniel Truhn, and Keno K Bresssem. 2023. [Medalpaca—an open-source collection of medical conversational ai models and training data](#). *arXiv preprint arXiv:2304.08247*.

Dan Hendrycks, Collin Burns, Steven Basart, Andy Zou, Mantas Mazeika, Dawn Song, and Jacob Steinhardt. 2020. Measuring massive multitask language understanding. *arXiv preprint arXiv:2009.03300*.

William Hiesinger, Cyril Zakka, Akash Chaurasia, Rohan Shad, Alex R. Dalal, Jennifer L. Kim, Michael Moor, Kevin Alexander, Euan A. Ashley, Jack Boyd, Kathleen Boyd, Karen Hirsch, Curt P. Langlotz, and Joanna Nelson. 2023. [Almanac: Retrieval-augmented language models for clinical medicine](#). *Research Square*.

Gautier Izacard, Patrick Lewis, Maria Lomeli, Lucas Hosseini, Fabio Petroni, Timo Schick, Jane Dwivedi-Yu, Armand Joulin, Sebastian Riedel, and Edouard Grave. 2022. Few-shot learning with retrieval augmented language models. *arXiv preprint arXiv:2208.03299*.

816	Ziwei Ji, Nayeon Lee, Rita Frieske, Tiezheng Yu, Dan Su, Yan Xu, Etsuko Ishii, Ye Jin Bang, Andrea Madotto, and Pascale Fung. 2023. Survey of hallucination in natural language generation. <i>ACM Computing Surveys</i> , 55(12):1–38.	872
817		873
818		874
819		875
820		876
		877
821	Di Jin, Eileen Pan, Nassim Oufattole, Wei-Hung Weng, Hanyi Fang, and Peter Szolovits. 2021. What disease does this patient have? a large-scale open domain question answering dataset from medical exams. <i>Applied Sciences</i> , 11(14):6421.	878
822		879
823		880
824		881
825		
826	Alistair Johnson, Lucas Bulgarelli, Tom Pollard, Steven Horng, Leo Anthony Celi, and Roger Mark. 2020. Mimic-iv. <i>PhysioNet</i> . Available online at: https://physionet.org/content/mimiciv/1.0/ (accessed August 23, 2021).	882
827		883
828		884
829		885
830		886
831	Sunjun Kweon, Junu Kim, Jiyoun Kim, Sujeong Im, Eunbyeol Cho, Seongsu Bae, Jungwoo Oh, Gyubok Lee, Jong Hak Moon, Seng Chan You, et al. 2023. Publicly shareable clinical large language model built on synthetic clinical notes. <i>arXiv preprint arXiv:2309.00237</i> .	887
832		888
833		
834		889
835		890
836		891
837	Yanis Labrak, Adrien Bazoge, Emmanuel Morin, Pierre-Antoine Gourraud, Mickael Rouvier, and Richard Dufour. 2024. Biomistral: A collection of open-source pretrained large language models for medical domains. <i>arXiv preprint arXiv:2402.10373</i> .	892
838		893
839		
840		894
841		895
842	Jinhyuk Lee, Wonjin Yoon, Sungdong Kim, Donghyeon Kim, Sunkyu Kim, Chan Ho So, and Jaewoo Kang. 2020. Biobert: a pre-trained biomedical language representation model for biomedical text mining. <i>Bioinformatics</i> , 36(4):1234–1240.	896
843		897
844		
845		898
846		899
847	Patrick Lewis, Ethan Perez, Aleksandra Piktus, Fabio Petroni, Vladimir Karpukhin, Naman Goyal, Heinrich Küttler, Mike Lewis, Wen-tau Yih, Tim Rocktäschel, et al. 2020. Retrieval-augmented generation for knowledge-intensive nlp tasks. <i>Advances in Neural Information Processing Systems</i> , 33:9459–9474.	900
848		901
849		902
850		903
851		904
852		
853	Xi Victoria Lin, Xilun Chen, Mingda Chen, Weijia Shi, Maria Lomeli, Rich James, Pedro Rodriguez, Jacob Kahn, Gergely Szilvasy, Mike Lewis, et al. 2023. Ra-dit: Retrieval-augmented dual instruction tuning. <i>arXiv preprint arXiv:2310.01352</i> .	905
854		906
855		907
856		908
857		909
858	Yun Luo, Zhen Yang, Fandong Meng, Yafu Li, Jie Zhou, and Yue Zhang. 2023. An empirical study of catastrophic forgetting in large language models during continual fine-tuning. <i>arXiv preprint arXiv:2308.08747</i> .	910
859		911
860		912
861		913
862		914
863		915
864	Sewon Min, Weijia Shi, Mike Lewis, Xilun Chen, Wen-tau Yih, Hannaneh Hajishirzi, and Luke Zettlemoyer. 2022. Nonparametric masked language modeling. <i>arXiv preprint arXiv:2212.01349</i> .	916
865		917
866		918
867		919
868		
869	Ankit Pal, Logesh Kumar Umapathi, and Malaikandan Sankarasubbu. 2022. Medmcqa: A large-scale multi-subject multi-choice dataset for medical domain question answering. In <i>Conference on Health, Inference, and Learning</i> , pages 248–260. PMLR.	920
870		921
871		922
		923
		924
	Cheng Peng, Xi Yang, Aokun Chen, Kaleb E Smith, Nima PourNejatian, Anthony B Costa, Cheryl Martin, Mona G Flores, Ying Zhang, Tanja Magoc, et al. 2023. A study of generative large language model for medical research and healthcare. <i>arXiv preprint arXiv:2305.13523</i> .	872
		873
		874
		875
		876
		877
	Fabio Petroni, Tim Rocktäschel, Patrick Lewis, Anton Bakhtin, Yuxiang Wu, Alexander H Miller, and Sebastian Riedel. 2019. Language models as knowledge bases? <i>arXiv preprint arXiv:1909.01066</i> .	878
		879
		880
		881
	Ohad Rubin, Jonathan Herzig, and Jonathan Berant. 2022. Learning to retrieve prompts for in-context learning . In <i>Proceedings of the 2022 Conference of the North American Chapter of the Association for Computational Linguistics: Human Language Technologies</i> , pages 2655–2671, Seattle, United States. Association for Computational Linguistics.	882
		883
		884
		885
		886
		887
		888
	Keshav Santhanam, Omar Khattab, Jon Saad-Falcon, Christopher Potts, and Matei Zaharia. 2021. Colbertv2: Effective and efficient retrieval via lightweight late interaction. <i>arXiv preprint arXiv:2112.01488</i> .	889
		890
		891
		892
		893
	Weijia Shi, Sewon Min, Michihiro Yasunaga, Minjoon Seo, Rich James, Mike Lewis, Luke Zettlemoyer, and Wen tau Yih. 2023. Replug: Retrieval-augmented black-box language models . <i>ArXiv</i> , abs/2301.12652.	894
		895
		896
		897
	Kurt Shuster, Spencer Poff, Moya Chen, Douwe Kiela, and Jason Weston. 2021. Retrieval augmentation reduces hallucination in conversation . In <i>Findings of the Association for Computational Linguistics: EMNLP 2021</i> , pages 3784–3803, Punta Cana, Dominican Republic. Association for Computational Linguistics.	898
		899
		900
		901
		902
		903
		904
	Karan Singhal, Shekoofeh Azizi, Tao Tu, S Sara Mahdavi, Jason Wei, Hyung Won Chung, Nathan Scales, Ajay Tanwani, Heather Cole-Lewis, Stephen Pfohl, et al. 2023a. Large language models encode clinical knowledge. <i>Nature</i> , 620(7972):172–180.	905
		906
		907
		908
		909
	Karan Singhal, Tao Tu, Juraj Gottweis, Rory Sayres, Ellery Wulczyn, Le Hou, Kevin Clark, Stephen Pfohl, Heather Cole-Lewis, Darlene Neal, et al. 2023b. Towards expert-level medical question answering with large language models. <i>arXiv preprint arXiv:2305.09617</i> .	910
		911
		912
		913
		914
		915
	Mujeen Sung, Jinhyuk Lee, Sean Yi, Minji Jeon, Sungdong Kim, and Jaewoo Kang. 2021. Can language models be biomedical knowledge bases? <i>arXiv preprint arXiv:2109.07154</i> .	916
		917
		918
		919
	Nandan Thakur, Nils Reimers, Andreas Ruckl’e, Abhishek Srivastava, and Iryna Gurevych. 2021. Beir: A heterogenous benchmark for zero-shot evaluation of information retrieval models . <i>ArXiv</i> , abs/2104.08663.	920
		921
		922
		923
		924

925	Augustin Toma, Patrick R Lawler, Jimmy Ba, Rahul G Krishnan, Barry B Rubin, and Bo Wang. 2023. Clinical camel: An open-source expert-level medical language model with dialogue-based knowledge encoding. <i>arXiv preprint arXiv:2305.12031</i> .	983
926		984
927		985
928		
929		
930	Hugo Touvron, Louis Martin, Kevin R. Stone, Peter Albert, Amjad Almahairi, Yasmine Babaei, Nikolay Bashlykov, Soumya Batra, Prajjwal Bhargava, Shruti Bhosale, Daniel M. Bikel, Lukas Blecher, Cristian Cantón Ferrer, Moya Chen, Guillem Cucurull, David Esiobu, Jude Fernandes, Jeremy Fu, Wenyin Fu, Brian Fuller, Cynthia Gao, Vedanuj Goswami, Naman Goyal, Anthony S. Hartshorn, Saghar Hosseini, Rui Hou, Hakan Inan, Marcin Kardas, Viktor Kerkez, Madian Khabsa, Isabel M. Kloumann, A. V. Korenev, Punit Singh Koura, Marie-Anne Lachaux, Thibaut Lavril, Jenya Lee, Diana Liskovich, Yinghai Lu, Yuning Mao, Xavier Martinet, Todor Mihaylov, Pushkar Mishra, Igor Molybog, Yixin Nie, Andrew Poulton, Jeremy Reizenstein, Rashi Rungta, Kalyan Saladi, Alan Schelten, Ruan Silva, Eric Michael Smith, R. Subramanian, Xia Tan, Binh Tang, Ross Taylor, Adina Williams, Jian Xiang Kuan, Puxin Xu, Zhengxu Yan, Iliyan Zarov, Yuchen Zhang, Angela Fan, Melanie Kambadur, Sharan Narang, Aurelien Rodriguez, Robert Stojnic, Sergey Edunov, and Thomas Scialom. 2023. Llama 2: Open foundation and fine-tuned chat models . <i>ArXiv</i> , abs/2307.09288.	986
931		987
932		988
933		989
934		990
935		991
936		
937		992
938		993
939		994
940		995
941		
942		996
943		997
944		998
945		999
946		1000
947		1001
948		
949		
950		1002
951		1003
952		1004
953	Hieu Tran, Zhichao Yang, Zonghai Yao, and Hong Yu. 2023. Bioinstruct: Instruction tuning of large language models for biomedical natural language processing. <i>arXiv preprint arXiv:2310.19975</i> .	1005
954		
955		
956		
957	Cunxiang Wang, Xiaoze Liu, Yuanhao Yue, Xiangru Tang, Tianhang Zhang, Cheng Jiayang, Yunzhi Yao, Wenyang Gao, Xuming Hu, Zehan Qi, et al. 2023. Survey on factuality in large language models: Knowledge, retrieval and domain-specificity. <i>arXiv preprint arXiv:2310.07521</i> .	1006
958		1007
959		1008
960		1009
961		1010
962		1011
963	Xuezhi Wang, Jason Wei, Dale Schuurmans, Quoc Le, Ed Chi, Sharan Narang, Aakanksha Chowdhery, and Denny Zhou. 2022. Self-consistency improves chain of thought reasoning in language models. <i>arXiv preprint arXiv:2203.11171</i> .	1012
964		1013
965		1014
966		1015
967		
968	Jason Wei, Xuezhi Wang, Dale Schuurmans, Maarten Bosma, Fei Xia, Ed Chi, Quoc V Le, Denny Zhou, et al. 2022. Chain-of-thought prompting elicits reasoning in large language models. <i>Advances in Neural Information Processing Systems</i> , 35:24824–24837.	1016
969		1017
970		1018
971		1019
972		1020
973	Michael Wornow, Yizhe Xu, Rahul Thapa, Birju S. Patel, Ethan H. Steinberg, S. Fleming, Michael A. Pfeffer, Jason A. Fries, and Nigam H. Shah. 2023. The shaky foundations of large language models and foundation models for electronic health records . <i>NPJ Digital Medicine</i> , 6.	1021
974		1022
975		1023
976		1024
977		
978		
979	Chaoyi Wu, Weixiong Lin, Xiaoman Zhang, Ya Zhang, Yanfeng Wang, and Weidi Xie. 2023. Pmc-llama: Towards building open-source language models for medicine. <i>arXiv preprint arXiv:2305.10415</i> , 6.	1025
980		1026
981		1027
982		1028
		1029
	Guangzhi Xiong, Qiao Jin, Zhiyong Lu, and Aidong Zhang. 2024. Benchmarking retrieval-augmented generation for medicine .	
	Zhichao Yang, Zonghai Yao, Mahbuba Tasmin, Parth Vashisht, Won Seok Jang, Feiyun Ouyang, Beining Wang, Dan Berlowitz, and Hong Yu. 2023. Performance of multimodal gpt-4v on usmle with image: Potential for imaging diagnostic support with explanations. <i>medRxiv</i> , pages 2023–10.	
	Zonghai Yao, Yi Cao, Zhichao Yang, and Hong Yu. 2022. Context variance evaluation of pretrained language models for prompt-based biomedical knowledge probing. <i>arXiv preprint arXiv:2211.10265</i> .	
	Michihiro Yasunaga, Antoine Bosselut, Hongyu Ren, Xikun Zhang, Christopher D Manning, Percy S Liang, and Jure Leskovec. 2022. Deep bidirectional language-knowledge graph pretraining. <i>Advances in Neural Information Processing Systems</i> , 35:37309–37323.	
	Ori Yoran, Tomer Wolfson, Ori Ram, and Jonathan Berant. 2023. Making retrieval-augmented language models robust to irrelevant context . <i>ArXiv</i> , abs/2310.01558.	
	Wenhao Yu. 2022. Retrieval-augmented generation across heterogeneous knowledge. In <i>Proceedings of the 2022 Conference of the North American Chapter of the Association for Computational Linguistics: Human Language Technologies: Student Research Workshop</i> , pages 52–58.	
	Li Yunxiang, Li Zihan, Zhang Kai, Dan Ruilong, and Zhang You. 2023. Chatdoctor: A medical chat model fine-tuned on llama model using medical domain knowledge. <i>arXiv preprint arXiv:2303.14070</i> .	
	Hongbo Zhang, Junying Chen, Feng Jiang, Fei Yu, Zhihong Chen, Jianquan Li, Guiming Chen, Xiangbo Wu, Zhiyi Zhang, Qingying Xiao, et al. 2023. Huatuogpt, towards taming language model to be a doctor. <i>arXiv preprint arXiv:2305.15075</i> .	
	Zhengyun Zhao, Qiao Jin, Fangyuan Chen, Tuorui Peng, and Sheng Yu. 2022. A large-scale dataset of patient summaries for retrieval-based clinical decision support systems . <i>Scientific Data</i> , 10.	
	Yutao Zhu, Huaying Yuan, Shuting Wang, Jiongnan Liu, Wenhan Liu, Chenlong Deng, Zhicheng Dou, and Ji-Rong Wen. 2023. Large language models for information retrieval: A survey. <i>arXiv preprint arXiv:2308.07107</i> .	

10 Appendix

10.1 Medical Corpus

Corpus	#Doc.
PubMed	23.9M
Textbooks	18
Cancer Care Ontario	87
Center for Disease Control and Prevention	621
Canadian Medical Association	431
International Committee of the Red Cross	49
National Institute for Health and Care Excellence	1.7k
Strategy for Patient-Oriented Research	217
World Health Organization	223
WikiDoc	33k

Table 5: For each medical corpus source, we provide the number of distinct documents, the approximate articles across all documents

10.2 MedQA Dataset

The MedQA dataset (Jin et al., 2021), sourced directly from the official USMLE website, included a range of sample questions for Step1, Step2CK, and Step3, released between June 2022 and March 2023. These questions represent the complex medical knowledge and ethical scenarios that medical students and practitioners are expected to navigate.

Additionally, Amboss question bank is a comprehensive resource widely used by medical professionals and students. This dataset provided an extensive array of Step1, Step2CK, and Step3-type questions, further enriching our training material with practical and diverse medical scenarios.

The MedMCQA dataset comprises 194k multiple-choice questions from Indian medical entrance exams, covering 2.4k healthcare topics and 21 medical subjects (Pal et al., 2022).

MMLU-Medical is selected from the MMLU dataset (Hendrycks et al., 2020), focused on nine subjects most pertinent to medical and clinical knowledge — high school biology, college biology, college medicine, professional medicine, medical genetics, virology, clinical knowledge, nutrition, and anatomy. Since this dataset has no training set, we opt to evaluate it using the LLM originally trained on MedMCQA.

We individually apply supervised finetuning on each QA dataset and subsequently assess their performance on the corresponding test sets, unless otherwise specified. MedQA and Amboss both offer detailed rationale with long explanations.

10.3 Baselines

For comparison with traditional domain pretraining method, we used Meditron, an open source LLM pretrained on clinical guidelines and research papers (Chen et al., 2023b). We also compared with other closed source LLMs such as OpenAI GPT-3.5, GPT-4 (Achiam et al., 2023), and Anthropic-Claude 3 (Anthropic, 2024). For the rationale evaluation experiment, we didn’t include Meditron because it cannot generate a valid rationale in our experiments. We didn’t include GPT-4 because it was used as the evaluator. To validate the benefit of joint training, we also compared JMLR with its naive version: RAG, which freezes the retriever and fetches the same document given a question.

10.4 Case Study

We presented four specific examples to further understand why JMLR outperforms other public models as shown in Table 7 and Table 8. The first three examples are from the Amboss dataset. Due to privacy concerns with Amboss, we cannot display the complete content of these questions. The last example is from a USMLE question. Our answers for the first two questions are correct, while GPT-3.5 responded incorrectly. Although both our model and GPT-3.5 answered the last two questions correctly, there were some differences in the rationale generated. For the first example, we found that JMLR’s retrieval function could extract similar questions, leading the model to answer incorrectly regarding direction. The retrieved document served as a background, fully utilizing the previously fine-tuned dataset. In the second example, we noticed that GPT-3.5 made a common-sense error: vaccination is not recommended for pregnant women in such cases. Even though GPT-3.5 has learned far more medical documents than our model by using pretraining or finetuning, it does not mean that the model will apply all medical knowledge correctly, even for some basic medical issues. In the third example, both we and GPT-3.5 answered correctly, but the rationale generated by GPT-3.5 differed significantly from the correct answer’s rationale: GPT-3.5 simply stated some facts without providing a logical reason. However, our model gave a more detailed and logical explanation of why there are decreased circulating T cells, as JMLR could retrieve related documents, such as some documents about SCID, to better understand the underlying principles. The last example

differs from the first three, as the highest-scoring document retrieved was from public guideline. The guideline provides a detailed introduction to PCOS and its symptoms, helping the model better explain. In contrast, GPT-3.5 simply correlated the symptoms straightforwardly without thoroughly analyzing other related symptoms, which can often lead to diagnostic errors, even though it answered this question correctly. Our model, however, performed a comprehensive analysis.

10.5 More Ablation Study

During training, we set the number of background documents to seven, maintaining this count during the inference phase as well. This quantity is optimal, according to our experiments, as illustrated in the figure 4. We employed the JMLR method to train the LLM on the MedQA dataset, retrieving varying numbers of documents. The performance is at its weakest when only one document is retrieved; this insufficiency leads to a lack of adequate medical knowledge for the model. As we increase the number of retrieved documents, the model’s performance gradually improves, reaching its peak with seven documents. However, once this number increases to ten, performance again declines due to retrieving an excess of irrelevant documents, which hinders the model’s ability to answer questions effectively.

To further demonstrate the applicability of our method across different large language models (LLMs), we conducted experiments on LLaMA 3 8B. In these experiments, we replaced the retrievable documents with training sets from other strong baselines. As shown in Table 6, our method (JMLR-8B) still achieved state-of-the-art (SOTA) performance, with scores of 74.7% on MedQA and 70.3% on MedMCQA. These results surpass other models, including Meerkat-8B and LLaMA-3-8B, further validating the effectiveness and generalizability of our approach.

Table 6: Model Performance on MedQA and MedMCQA

Model	MedQA (%)	MedMCQA (%)
Meerkat-8B	74.0	62.7
Self-BioRAG-7B	48.6	44.0
BioMistral-7B	50.6	48.1
LLaMA-3-8B	64.9	68.5
JMLR-8B (Ours)	74.7	70.3

10.6 Training Resource

In our study, we utilized various training resources to evaluate the performance of different models on medical question-answering (QA) datasets. According to the data, for MedQA datasets, JMLR-13B, which requires 148 GPU hours for training, significantly outperforms Meditron-70B, which necessitates 42,630 GPU hours. In comparison, JMLR-7B needs approximately 100 GPU hours, RAG-7B requires 72 GPU hours, and RAG-13B needs 128 GPU hours.

The training time for JMLR models is considerably lower than that for Meditron-70B, though slightly higher than RAG-13B. However, JMLR models achieve state-of-the-art (SOTA) performance. Interestingly, we observe a substantial performance improvement in RAG-13B compared to RAG-7B. This improvement can be attributed to the fact that RAG models struggle to effectively learn how to understand or utilize medical documents. As a result, the performance of RAG-7B is limited by its model size. Conversely, RAG-13B, with its increased model size, is better able to comprehend documents, leading to enhanced performance. Our JMLR models, on the other hand, excel in enabling the model to understand and utilize medical documents effectively. This capability is reflected in their SOTA performance across multiple datasets, demonstrating the efficacy of our approach in medical QA tasks.

10.7 Training Details

Both our training process and the conventional finetuning approach employ the AdamW optimizer, with $\beta_1 = 0.9$, $\beta_2 = 0.95$, and $\text{eps} = 1 \times 10^{-5}$. We implement a cosine learning rate schedule, incorporating a warmup phase that accounts for 10% of the training duration and decays the learning rate to 10% of its peak value. In alignment with the practices outlined in Llama 2-chat (Touvron et al., 2023), our training employs a learning rate of 1×10^{-5} , a weight decay factor of 0.1, and manages a batch size of 2. The finetuning phase spans 5 epochs for all iterations. However, we apply a distinct learning rate for ColBERT, set at $3e - 5$. The optimization strategy for training ColBERT mirrors that used for Llama 2. Throughout these experiments, we utilize four A100 80 GB GPUs.

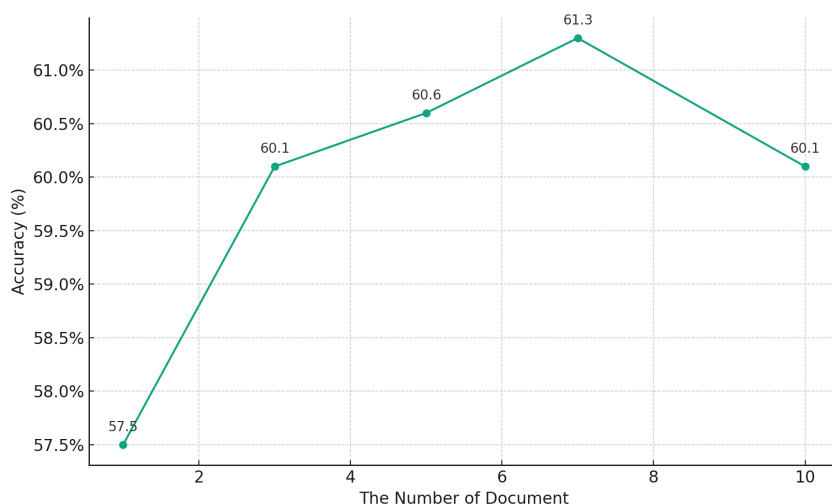


Figure 4: The horizontal axis represents the number of documents retrieved in JMLR, while the vertical axis shows the accuracy of JMLR tested on the USMLE.

10.8 Factuality metrics: UMLS-F1

The assessment of factual accuracy in LLMs output leverages the UMLS concept overlap metric. The Unified Medical Language System (UMLS), established by (Bodenreider, 2004), significantly contributes to the biomedical domain’s interoperability. It achieves this by amalgamating and disseminating a comprehensive collection of biomedical terminologies, classification systems, and coding standards from many sources. By doing so, UMLS aids in reconciling semantic variances and representational disparities found across different biomedical concept repositories.

For the identification and alignment of medical named entities within texts to their corresponding biomedical concepts in UMLS, we employed the Scispacy library³. Scispacy excels in identifying and clarifying entities, thus facilitating the accurate association of named entities found in LLMs output with the relevant UMLS concepts. This capability is critical for evaluating the LLMs output’s factual accuracy.

The analytical process for LLMs output utilizes metrics of precision and recall. Precision represents the ratio of concepts present in both the LLM output and ground truth content, serving as a measure of the LLM output’s factual correctness. In contrast, recall evaluates how well the information in the LLM output matches the intended content, reflecting the relevance of the presented informa-

tion.

To calculate these metrics, we consider the concept sets from both the ground truth (C_{ref}) and the LLM output (C_{gen}). The formulas for recall and precision are as follows:

$$\text{Recall} = \frac{|C_{ref} \cap C_{gen}|}{|C_{ref}|}$$

$$\text{Precision} = \frac{|C_{ref} \cap C_{gen}|}{|C_{gen}|}$$

The F1 score, derived from the above precision and recall values, is reported to provide a balanced measure of LLMs output’s accuracy and relevance.

10.9 Prompt for Evaluation

For GPT-4 evaluation, we assessment each result from three ways: comprehension, reasoning step and recall of knowledge. The prompt is shown in Table 9

³We used the Scispacy *en_core_sci_lg* model.

Q1: A 48-year-old man...

Answer:

GPT-3.5:

The correct answer is A) Cerebral edema.

Explanation: This patient presents with symptoms consistent with alcohol withdrawal syndrome (AWS), which can manifest as seizures (alcohol withdrawal seizures) due to abrupt cessation or reduction of alcohol intake in a chronic heavy drinker. AWS seizures typically occur within 48 hours of reducing alcohol intake.

This patient's laboratory findings are indicative of hyponatremia (low serum sodium), which is common in severe alcohol withdrawal due to the syndrome of inappropriate antidiuretic hormone secretion (SIADH). SIADH leads to water retention and dilutional hyponatremia.

The risk of cerebral edema is increased in patients with severe hyponatremia who are rapidly corrected to normal serum sodium levels. Rapid correction of hyponatremia can lead to osmotic shifts of water into the brain cells, causing cerebral edema, which may result in neurological deterioration, seizures, coma, and death. This risk is particularly high in chronic alcoholics due to adaptive changes in brain osmolytes.

Given the patient's current status, urgent treatment to normalize serum sodium levels (such as with hypertonic saline infusion) puts him at increased risk for cerebral edema. Therefore, careful monitoring and slow correction of hyponatremia are essential in this patient to avoid this potentially fatal complication.

Our:

This patient's presentation is consistent with alcohol withdrawal syndrome (AWS), which is characterized by autonomic hyperactivity, tremulousness, and seizures. AWS can occur in patients with a history of chronic alcohol use disorder who abruptly stop drinking or significantly reduce their alcohol intake. The syndrome is thought to be due to the withdrawal of the inhibitory effects of alcohol on the central nervous system.

The most common complication of AWS is seizures, which can occur within 48 hours of the last drink. Seizures are often generalized tonic-clonic seizures and can be life-threatening. Other complications include delirium tremens (DTs), which is characterized by hallucinations, confusion, and autonomic instability. DTs can also lead to seizures and death.

The treatment of AWS involves supportive care, including hydration, benzodiazepines, and possibly antipsychotics. In severe cases, hospitalization may be necessary for close monitoring and management of complications.

Osmotic myelinolysis (also known as central pontine myelinolysis) is a condition that can occur in patients with severe hyponatremia (low sodium levels in the blood) who are treated with rapid correction of their sodium levels. This condition is characterized by demyelination of the central nervous system, leading to neurologic symptoms such as confusion, seizures, and coma.

Given the patient's presentation and history of chronic alcohol use disorder, the most appropriate treatment is supportive care for AWS, including hydration, benzodiazepines, and possibly antipsychotics. Rapid correction of his sodium levels is not indicated due to the risk of osmotic myelinolysis.

Expertise Comment: *GPT-3.5 incorrectly interpreted the patient's symptoms as primarily related to Alcohol Withdrawal Syndrome (AWS) without adequately considering the patient's laboratory results, particularly the severe hyponatremia (serum sodium 112 mEq/L). Although seizures can indeed accompany AWS, in this case, the diagnosis and treatment of hyponatremia should be the primary focus. Moreover, it incorrectly associated the risks of rapid correction of hyponatremia with cerebral edema. In fact, the main risk of rapidly correcting hyponatremia is osmotic myelinolysis, not cerebral edema. Osmotic myelinolysis results from rapid changes in blood osmolarity, leading to damage to the myelin sheath of brain neurons.*

Retrieve: A 48-year-old man is brought to the emergency department by his wife 20 minutes after she witnessed him vigorously shaking for about 1 minute. During this episode, he urinated on himself. He feels drowsy and has nausea. He has a history of chronic alcoholism; he has been drinking 15 beers daily for the past 3 days. Before this time, he drank 8 beers daily. His last drink was 2 hours ago. He appears lethargic. His vital signs are within normal limits. Physical and neurologic examinations show no other abnormalities. On mental status examination, he is confused and not oriented to time. Laboratory studies show: Hematocrit 44.0% Leukocyte count 12,000/mm³ Platelet count 320,000/mm³ Serum Na⁺ 112 mEq/L Cl⁻ 75 mEq/L K⁺ 3.8 mEq/L HCO₃⁻ 13 mEq/L Urea nitrogen 6 mEq/L Creatinine 0.6 mg/dL Albumin 2.1 g/dL Glucose 80 mg/dL Urgent treatment for this patient's current condition puts him at increased risk for which of the following adverse events? A: Cerebral edema B: Cardiac arrhythmia C: Hyperglycemia D: Osmotic myelinolysis E: Wernicke encephalopathy
Correct Answer: D

Q2: A 27-year-old gravida 2, para 1 comes...

Answer:

GPT-3.5:

Based on the clinical presentation described, the most likely diagnosis for this patient is Rubella (German measles) infection during pregnancy, which can lead to congenital rubella syndrome (CRS) in the fetus if contracted during the first trimester. The typical symptoms of rubella include a maculopapular rash starting on the face and spreading downwards, along with lymphadenopathy and joint swelling.

Given the risk of congenital rubella syndrome to the fetus, the most appropriate next step in management is:

C) Vaccination

Vaccination against rubella is contraindicated during pregnancy due to the risk of causing CRS. However, after delivery, the patient should receive the rubella vaccine to prevent future infections. This will not only protect the patient from future rubella infections but also prevent the risk of transmitting the virus to others, including vulnerable populations such as pregnant women.

Options A, D, and E are not appropriate in this scenario. Oral acyclovir therapy (Option A) is used for herpes simplex virus infections, not rubella. Reassurance and symptomatic therapy (Option D) may provide comfort but do not address the potential risk to the fetus. Intravenous immunoglobulin therapy (Option E) is not indicated for rubella infection during pregnancy. Termination of pregnancy (Option B) is not necessary unless there are severe fetal abnormalities detected on further evaluation.

Our:

The patient's history of a rash that started on her face and progressed downwards, along with the presence of postauricular lymphadenopathy, is suggestive of rubella infection. Rubella is a highly contagious viral infection that is spread through respiratory droplets or direct contact with infected secretions. It is characterized by a prodrome of malaise, low-grade fever, and lymphadenopathy, followed by the appearance of a pink maculopapular rash that begins on the face and spreads downwards. The rash is usually itchy and lasts for 3-5 days.

Rubella infection during pregnancy, especially during the first trimester, can have serious consequences for the developing fetus. It can cause congenital rubella syndrome (CRS), which is characterized by a wide range of birth defects, including cataracts, deafness, heart defects, and intellectual disability.

The most appropriate next step in management for this patient is termination of pregnancy. This is because the risk of CRS is high if the fetus is exposed to rubella during the first trimester, and the risk of birth defects outweighs the potential benefits of continuing the pregnancy.

Options A, B, C, and E are not appropriate in this case. Acyclovir is used to treat herpes simplex virus infections, not rubella. Vaccination is not recommended during pregnancy due to the risk of fetal infection. Reassurance and symptomatic therapy are not sufficient to prevent the risk of CRS. Intravenous immunoglobulin therapy is not indicated for rubella infection during pregnancy.

Expertise Comment: GPT-3.5 made a basic error; it's not appropriate to vaccinate during pregnancy.

Table 7: Case Study For Retrieval Documents.

Q4: A 1-year-old girl is brought to the physician...

Answer:

GPT-3.5:

Given the clinical presentation and findings described, this patient is most likely suffering from severe combined immunodeficiency (SCID), which is characterized by a deficiency in both T and B lymphocytes. The additional finding most likely to be present in this patient with SCID is: D) Decreased circulating T cells. SCID is a primary immunodeficiency disorder characterized by profound defects in both cellular and humoral immunity. Patients with SCID typically have absent or markedly reduced T cell counts, as T cell development and function are severely impaired. This deficiency in T cells predisposes patients to recurrent, severe, and often life-threatening infections. While B cells may also be affected in SCID, the absence of T cells is the primary hallmark of the disease. Therefore, decreased circulating T cells (Option D) would be the most likely additional finding in this patient. Other options such as increased circulating IgE (Option B) or increased circulating neutrophils (Option F) are less specific to SCID and could be seen in a variety of other conditions.

Our:

Correct Answer: D Decreased circulating T cells

This patient's severe combined immunodeficiency (SCID) is most likely due to an autosomal recessive adenosine deaminase deficiency (the second most common cause of SCID), which results in disrupted purine metabolism and accumulation of metabolites (including deoxyadenosine and dATP) that are toxic to maturing lymphocytes. Accumulation of dATP also inhibits the function of ribonucleotide reductase, which is essential for the generation of deoxynucleotides, thereby impairing the proliferation of lymphocytes. These effects on lymphocytes proliferation and maturation lead to a decreased number of circulating T cells, B cells, and NK cells, resulting in both cellular and humoral immunodeficiency. Clinically, patients with SCID have no tonsils, no palpable lymph nodes, and a rudimentary thymus. In contrast, X-linked SCID (the most common variant) is caused by a defect in the IL-2 receptor, which is required for T-cell proliferation. Thus, X-linked SCID manifests with a decrease in circulating T cells and a normal number of B cells. Congenital immunodeficiency disorders

Decreased levels of circulating parathyroid hormone in association with immunodeficiency can be seen in patients with DiGeorge syndrome. This syndrome also manifests with thymic hypoplasia and, possibly, the absence of tonsils. However, other features of CATCH-22 (e.g., congenital heart disease, dysmorphic facial features, hypocalcemia) would also be expected. Increased deoxyadenosine concentration in both the serum and urine and absent tonsils are not associated with DiGeorge syndrome. Increased circulating IgE levels can be seen in patients with Job syndrome, which is an immunodeficiency characterized by impaired neutrophil recruitment to the site of infection. Further manifestations would typically include coarse facial features, eosinophilia, severe eczema, and recurrent abscess formation. Increased deoxyadenosine concentration in both the serum and urine, absent tonsils, and an absent thymic shadow on x-ray are not associated with Job syndrome. Circulating B cells are decreased (not increased) in SCID due to adenosine deaminase deficiency and in X-linked agammaglobulinemia, an immunodeficiency characterized by a defective Bruton tyrosine kinase gene. Although X-linked agammaglobulinemia can also present with recurrent, severe pyogenic infections beginning > 4–6 months after birth, it is extremely rare in girls given its mode of inheritance. Absent thymic shadow, tonsillar hypoplasia, and elevated deoxyadenosine levels are also not consistent with this diagnosis. In X-linked SCID (the most common variant), the number of circulating B cells is normal. This patient's severe combined immunodeficiency (SCID) is most likely due to an autosomal recessive adenosine deaminase deficiency (the second most common cause of SCID), which results in disrupted purine metabolism and accumulation of metabolites (including deoxyadenosine and dATP) that are toxic to maturing lymphocytes. Accumulation of dATP also inhibits the function of ribonucleotide reductase, which is essential for the generation of deoxynucleotides, thereby impairing the proliferation of lymphocytes. These effects on lymphocytes proliferation and maturation lead to a decreased number of circulating T cells, B cells, and NK cells, resulting in both cellular and humoral immunodeficiency. Clinically, patients with SCID have no tonsils, no palpable lymph nodes, and a rudimentary thymus. In contrast, X-linked SCID (the most common variant) is caused by a defect in the IL-2 receptor, which is required for T

Expertise Comment: GPT-3.5's explanation of the pathology is unclear, such as the specific type of SCID (Severe Combined Immunodeficiency caused by adenosine deaminase deficiency) and how this condition affects the proliferation and maturation of lymphocytes, leading to a reduced number of T cells.

Retrieve: ...The treatment for mild to moderate cases is mainly supportive, with early treatment of infections and prophylaxis with trimethoprim-sulfamethoxazole if needed, but severe cases require definitive therapy with hematopoietic stem cell transplantation. Congenital immunodeficiency disorders A defect in the interleukin-2 receptor subunit gamma gene (IL2RG) is the most common mutation associated with severe combined immunodeficiency (SCID), which can manifest soon after birth with recurrent episodes of otitis media, candidiasis, and sepsis. However, patients would also typically show failure to thrive and have a history of chronic diarrhea. A CBC, moreover, would reveal a low absolute lymphocyte count (< 1000/mm³). Delayed umbilical cord separation would not be expected. A defect in Bruton tyrosine kinase (BTK) is responsible for X-linked agammaglobulinemia (XLA), which may result in recurrent otitis media from infection with extracellular bacteria such as *S. pneumoniae* and *H. influenzae*. However, infants with B-cell defects such as XLA typically do not develop symptoms before 320136 months because they generally retain passively acquired maternal antibodies up to this age. Delayed umbilical cord separation would also not be expected. Moreover, candidiasis is more commonly seen in defects involving T cells and granulocytes than in isolated primary defects of antibody production such as XLA. Defective NADPH oxidase results in chronic granulomatous disease (CGD), which may manifest in infancy with candidiasis (since *C. albicans* is catalase-positive) and neutrophilia during episodes of infection. However, these infections tend to remain localized, and sepsis is not as common as in other primary immune deficiency syndromes. Other pathognomonic features of CGD include GI obstruction and urinary retention caused by granulomas. Delayed umbilical cord separation would not be expected. Defective microtubules due to a loss of function of the lysosomal trafficking regulator gene (LYST) is the underlying pathophysiology of Chediak-Higashi syndrome (CHS), which can result in systemic candidiasis. However, patients with CHS would have neutropenia, not neutrophilia. Features such as oculocutaneous albinism and/or ocular motility disorders (e.g., strabismus, nystagmus) would also be present. Delayed umbilical cord separation would not be expected. A defectively organized actin cytoskeleton due to a mutation in the WAS gene is the underlying cause of Wiskott-Aldrich syndrome (WAS), which can manifest in infancy with recurrent otitis media as well as scaly erythematous lesions in the diaper area due to atopic dermatitis. However, the absence of thrombocytopenia on a CBC essentially rules out WAS. Delayed umbilical cord separation would also not be expected...

Table 8: Case Study For Retrieval Documents

1 Q3: A 27-year-old woman presents to the office with concerns about her long struggle with her physical appearance since adolescence. She says she has always been large and was constantly targeted by her classmates and coworkers for being so. Her main concern at the moment is her acne and unwanted facial hair on her upper lip, for which she often visits a local spa. She has tried numerous diet plans, exercise regimens, and cosmetic products with little to no effect. Recently, she underwent a glucose tolerance test that showed a plasma glucose level of 160 mg/dL (8.9 mmol/L) after 2 hours of a 75 g dose of oral glucose. She has a family history of type 2 diabetes mellitus and a menstrual cycle that occurs every 45 days. Her pulse is 72/min and the blood pressure is 138/80 mm Hg. On physical examination, her height is 160 cm (5 ft 3 in) and her weight is 85 kg (187 lb), and she has severe inflammatory acne over the cheeks and forehead and dark coarse hairs on the back. What is the most likely diagnosis of this patient? A: Hypothyroidism B: Idiopathic hirsutism C: Cushing's disease D: Polycystic ovarian syndrome (PCOS) E: Ovarian hyperthecosis

Answer:

GPT-3.5:

The most likely diagnosis for this patient is: D: Polycystic ovarian syndrome (PCOS) PCOS is a common endocrine disorder in women of reproductive age, characterized by hyperandrogenism, irregular menstrual cycles, and polycystic ovaries on ultrasound. The clinical features seen in this patient, including acne, unwanted facial hair (hirsutism), obesity, irregular menstrual cycles, and a family history of type 2 diabetes mellitus, are all consistent with PCOS. Other options: A: Hypothyroidism - While hypothyroidism can present with weight gain and menstrual irregularities, it is less likely given the presence of hirsutism and obesity in this patient. B: Idiopathic hirsutism - This is unlikely as idiopathic hirsutism typically presents with hirsutism without other features of PCOS such as irregular menstrual cycles and obesity. C: Cushing's disease - While Cushing's disease can present with weight gain and hirsutism, it is less likely in this patient as there are no signs of hypercortisolism such as central obesity, buffalo hump, or purple striae. E: Ovarian hyperthecosis - This is a rare condition characterized by luteinization of ovarian stromal cells leading to hyperandrogenism. However, PCOS is a more common cause of hirsutism and irregular menstrual cycles in young women.

Our:

The patient's history of being "large" since adolescence, a family history of type 2 diabetes mellitus, and a menstrual cycle that occurs every 45 days, along with her physical examination findings of severe inflammatory acne over the cheeks and forehead and dark coarse hairs on the back, are suggestive of polycystic ovary syndrome (PCOS). PCOS is a common endocrine disorder among women of reproductive age and is characterized by hyperandrogenism, chronic anovulation, and polycystic ovaries on ultrasound. The condition is associated with insulin resistance, which can lead to hyperglycemia and impaired glucose tolerance, as seen in this patient's glucose tolerance test.

The other options listed are not as likely given the patient's presentation:

A: Hypothyroidism is characterized by a slowing of metabolic processes, including growth and development, and is not associated with the symptoms or findings seen in this patient.

B: Idiopathic hirsutism is a condition characterized by excessive hair growth in women, often on the face, chest, and back, but it does not typically present with the other symptoms or findings seen in this patient.

C: Cushing's disease is a condition caused by excessive production of cortisol, which can lead to weight gain, central obesity, and facial rounding, but it does not typically present with the other symptoms or findings seen in this patient.

D: Polycystic ovarian syndrome (PCOS) is a common endocrine disorder among women of reproductive age and is characterized by hyperandrogenism, chronic anovulation, and polycystic ovaries on ultrasound. The condition is associated with insulin resistance, which can lead to hyperglycemia and impaired glucose tolerance, as seen in this patient's glucose tolerance test.

E: Ovarian hyperthecosis is a condition characterized by excessive production of androgens by the ovaries, which can lead to hirsutism and acne, but it does not typically present with the other symptoms or findings seen in this patient.

Expertise Comment: Our explanation is slightly more detailed in terms of linking the patient's specific symptoms to the characteristics of PCOS and explaining why other diagnoses are less likely. It provides a more comprehensive understanding of PCOS and its relation to the patient's symptoms and test results. On the other hand, GPT-3.5 offers a more concise but still accurate diagnosis.

GPT-4 **System**
"Act as a USMLE evaluator, your role involves assessing and comparing a medical student's explanation to the provided target answer. Begin the assessment by carefully reviewing the provided target answer. Then, based on following specific criteria, determine the score for the student's answer."

Evaluation Criteria
"For each diagnosis, evaluate the medical student explanation base on the following three questions:"

Question 1
"Does the medical student's answer contain any evidence of incorrect reading comprehension? (indication the question has not been understood)"

Question 2
"Does the medical student's answer contain any evidence of incorrect reasoning steps? (incorrect rationale for answering the question)"

Question 3
"Does the medical student's answer contain any evidence of incorrect recall of knowledge? (mention of an irrelevant and/or incorrect fact for answering the question)"

Input "Medical student's answer: Reason generated by model
"Medical student's answer: Reason generated by model
"Target answer: Ground truth reason
"Background Question: Question

Output Format "Your evaluation should be provided in JSON format, as follows(don't generate any other information):
{"case 1": {"question 1": "The score for question 1", "question 2": "The score for question 2", "question 3": "The score for question 3"}, "case 2": "score for case 2 with the same format as case 1", "case 3": "score for case 3 with the same format as case 1", "overall score": "the average score for question 1, 2, 3", "reason": "the reason why you give the score"}}

Table 9: Evaluation Prompt for GPT-4.

		MMLU	MedMCQA	MedQA	Amboss	Average
Non Corpus	PMC-Llama-7B	59.7	57.6	42.4	43.7	50.9
	Llama 2-7B	56.3	54.4	44.0	46.5	50.3
	Meditron-7B	55.6	59.2	47.9	50.1	53.2
	ChatGPT	69.4	51.0	50.2	49.1	54.9
	Meditron70B	73.6	65.1	60.7	76.4	68.9
Open Guidelines	RAG-7B	63.8	62.1	47.3	50.7	55.9
	RAG-13B	69.8	63.4	56.8	60.7	62.7
	RAG-ChatGPT	68.9	55.2	53.3	49.3	56.7
	JMLR-7B	65.3	64.1	51.3	68.3	62.3
	JMLR-13B	70.1	64.5	59.5	79.6	68.4
All Corpus	RAG-7B	62.1	62.4	54.6	70.7	62.5
	RAG-13B	69.9	64.2	59.9	76.9	67.7
	JMLR-ChatGPT	70.1	55.3	54.3	50.1	57.5
	JMLR-7B	64.3	64.2	56.2	71.2	64.0
	JMLR-13B	72.8	65.5	62.5	81.2	70.5
MedRAG Corpus	MedRAG-ChatGPT	75.5	58.0	53.6	48.8	59.0

Table 10: Since Meditron-70B has already been tested on MedQA, we are directly using its results (Chen et al., 2023b). For ChatGPT, we utilized the API of GPT-3.5-turbo to conduct tests on both MedQA and Amboss datasets. For RAG-7B and RAG-13B, we employed the same medical guidelines and medical QA bank that we used with JMLR.